Structural Engineering and Mechanics, Vol. 18, No. 2 (2004) 211-229
DOI: http://dx.doi.org/10.12989/sem.2004.18.2.211

Non linear seismic response of a low reinforced concrete structure : modeling by multilayered finite shell elements

J. F. Semblat†

Laboratoire Central des Ponts et Chaussées (LCPC), Eng. Modeling Department, 58 bd Lefebvre, 75732 PARIS Cedex 15, France

A. Aouameur‡

Dassault Data Services, Formerly at Laboratoire Central des Ponts et Chaussées (LCPC), France

F. J. Ulm‡†

Massachusetts Institute of Technology, Cambridge, USA

(Received October 29, 2003, Accepted March 10, 2004)

Abstract. The main purpose of this paper is the numerical analysis of the non-linear seismic response of a RC building mock-up. The mock-up is subjected to different synthetic horizontal seismic excitations. The numerical approach is based on a 3D-model involving multilayered shell elements. These elements are composed of several single-layer membranes with various eccentricities. Bending effects are included through these eccentricities. Basic equations are first written for a single membrane element with its own eccentricity and then generalised to the multilayered shell element by superposition. The multilayered shell is considered as a classical shell element : all information about non-linear constitutive relations are investigated at the local scale of each layer, whereas balance and kinematics are checked afterwards at global scale. The non-linear dynamic response of the building is computed with Newmark algorithm. The numerical dynamic results (blind simulations) are considered in the linear and non linear cases and compared with experimental results from shaking table tests. Multilayered shell elements are found to be a promising tool for predictive computations of RC structures behaviour under 3D seismic loadings. This study was part of the CAMUS International Benchmark.

Key words: structural dynamics; non linear seismic response; multilayered shells; 3D modeling; finite element method.

1. Introduction

The analysis of the dynamic response of structures under seismic excitation can be performed through various means at different scales. In this paper, we analyze the behaviour of a low-reinforced concrete structure at a detailed scale considering a multilayered finite shell element. The

† Researcher
‡† Professor

experimental analysis has been performed through reduced scale tests within the framework of the CAMUS project (CEA 1997, 1998). A prerequisite for predicting the response of the complex systems subjected to earthquake excitation, is the comprehensive understanding of the response of its various components by means of numerical simulations. We therefore present here the contribution of our laboratory (LCPC, France) to this project through the numerical modeling (blind simulation) of the non linear seismic response of the structure. This study should allow the validation of the multilayered shell element for a specific type of loading and could lead afterwards to various simulations for various types of structures and complex seismic excitations.

2. Seismic response of structures

2.1 Structural dynamics

The analysis of the seismic response of structures or dynamic soil-structure interaction can be investigated through many various numerical or experimental methods from simplified ones (Bisch 1999, Chopra 2002, Clough 1993, Fajfar 2000, Pauley 1992, Semblat 1997) to rather complex ones (Aouameur 1998, Ile 1998, Lin 1975, Mazars 1990, 1998, Polak 1993, Ragueneau 1998, Semblat 2002a,b, Sercombe 1998, Thomas 1995, Ulm 1993a, 1994). The main point is the efficiency of the method in question towards its accuracy to analyze the problem. The numerical method presented hereafter is a rather sophisticated tool mainly adapted for the analysis of complex structures under various seismic loadings. A crucial aspect of the problem is often the precise knowledge of the seismic loading which depends on such various phenomena as site effects (Bard 1985, Guéguen 2000, Semblat 1998a, 2000), non linear soil behaviour (Aubry 1992, Garnier 1999, Seed 1986).

2.2 The CAMUS project

The CAMUS project aims at comparing and validating the numerical tools commonly used for the load bearing walls thanks to shaking table experiments. This project was supported by several French authorities and companies : Commissariat à l'Energie Atomique (CEA), Fédération Nationale du Bâtiment (FNB), Plan Génie Civil and Electicité De France (EDF). The experimental program took place in the CEA facilities in Saclay (France) and 11 international teams (Canada, Europe, Japan, USA) participated to CAMUS numerical benchmark through blind simulations (CEA 1997, CEA 1998). A reduced-scale model of the structure was considered and tested on the Azalée shaking table (CEA 1997, Semblat 1999).

Other french research programs were previously made on earthquake performance of RC structures as for example « CASSBA » (Mazars 1998, Semblat 1999). Recent developments of the CAMUS project also concern soil structure interaction and performance of EC8 designed structures.

3. Shaking table experiments and numerical modeling

3.1 Reduced scale model

The reduced scale (1/3rd) model considered for the shaking table tests within the CAMUS project

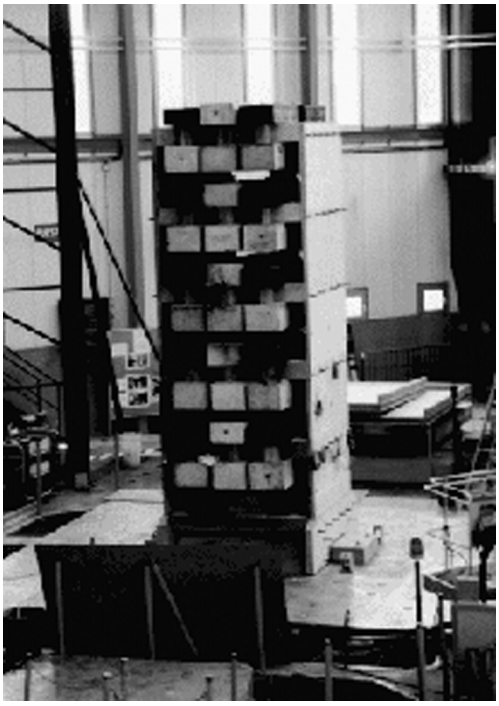

Fig. 1 Low reinforced concrete structure CAMUS on the “Azalée” shaking table (CEA)

is the mock-up of a low reinforced concrete structure (CEA 1997, Mazars 1998). This structure is designed according to the french codes. As shown in Fig. 1, it is composed of two parallel R/C walls without openings, linked by 6 square floors (including the floor connected to the footing). A heavily reinforced concrete footing allows the anchorage to a shaking table. The walls are loaded in their own plane. The stiffness and the strength in the perpendicular direction are increased by adding some lateral triangular bracing. This system reduces the risk of failure which might be induced by some parasite transversal motion or a non-symetric failure of the structural walls. As shown in Fig. 1, the total mass of each floor includes the self weight of the floor and 6 additional masses (above and under the floor) (Semblat 1999). These masses have been determined in order to impose a normal force to the walls compatible with the vertical stress values commonly found at the base of such structures (i.e., scale factors of the dynamic reduced scale model).

3.2 Shaking table experiments

The RC mock-up is anchored to the « Azalée » shaking table and several experiments are performed. Firstly, the determination of the eigenmodes of the structure is made using low level random excitation. Afterwards, horizontal moderate and strong seismic excitations are applied on the shaking table. The features of the dynamic loadings are given in the following sections. For the numerical benchmark, the only information are both geometrical and mechanical features (determined from laboratory tests on concrete specimens) as well as the first three eigenmodes of the structure (estimated from the low level random excitation tests). From these informations, one has to model the non linear seismic reponse of the whole structure (blind simulations).

3.3 Numerical modeling

In this article, the modelling and analysis of CAMUS structure are considered. A three-dimensional model, based on a mutilayered shell element formulation, is used. This formulation allows to take into account material and geometrical non linear effects in the structural analysis of shell structures subject to various loadings (Aouameur 1998, 1999). Only the material nonlinearities are considered in this paper since geometrical ones have no significant influence in the behaviour of such a structure. 2D models were also considered in the study (Semblat 1998b) but are not presented herein.

The determination of the dynamic response is made using the general finite element code CESAR-LCPC (Humbert 1989). The non linear response of the structure is estimated thanks to a numerical model including multilayered finite shell elements (implemented in CESAR-LCPC). The theoretical formulation of these elements is presented hereafter.

4. Multilayered shell element

4.1 General presentation

The multilayered shell element developed is composed of several single-layer membranes with various eccentricities and thicknesses (Fig. 2). Bending effects are included through these eccentricities. There are many links between local and global scales. All information about non-linear constitutive relations are investigated at the local scale of each layer, whereas balance and kinematics are checked afterwards at global scale.

The main idea consists in establishing basic equations for a single membrane element with its own eccentricity and behaviour. These equations are then generalised to the multilayered shell element by superposition, according to specific assumptions.

Denoting $\hat{\mathbf{U}}_0$ and $\hat{\mathbf{\Omega}}_0$ any vectorial fields of displacement and rotation, we make the assumption of small perturbations. The local dynamic equilibrium, expressed as force and moment, of a shell of thickness h moved away from the reference surface S is leading to the following equations (Aouameur 1998, 1999):

$$\frac{\partial(B\mathbf{N}_\alpha)}{\partial\alpha} + \frac{\partial(A\mathbf{N}_\beta)}{\partial\beta} + AB(\mathbf{q} - \rho h\ddot{\mathbf{U}}_0 - \rho e h\ddot{\mathbf{\Omega}}_0) = 0 \tag{1}$$

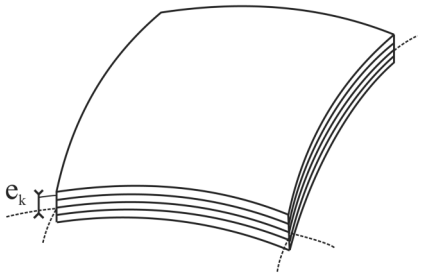

Fig. 2 Multilayered finite shell element for the semi-global formulation: global kinematics for the shell element with local analysis of the constitutive behaviour in each layer

$$\frac{\partial(B\mathbf{M}_\alpha)}{\partial\alpha} + \frac{\partial(A\mathbf{M}_\beta)}{\partial\beta} + AB(\mathbf{n}_\alpha \wedge \mathbf{N}_\alpha + \mathbf{n}_\beta \wedge \mathbf{N}_\beta + \mathbf{m} - \mathbf{I}\cdot\ddot{\boldsymbol{\Omega}}_0 - \rho eh\ddot{\mathbf{U}}_0) = 0 \tag{2}$$

where $\mathbf{q}$ and $\mathbf{m}$ are respectively the force and moment applied by surface unit; $\mathbf{n}_\alpha$ and $\mathbf{n}_\beta$ the local basis vectors of the shell; $\mathbf{N}_\alpha$, $\mathbf{N}_\beta$, $\mathbf{M}_\alpha$ and $\mathbf{M}_\beta$ the forces (with normal and shear components) and global moments by length unit; ρ and e the mass density and eccentricity of the shell; A and B the *Lamé* parameters and I the dynamic moment of inertia defined by:

$$I = \int_{e-h/2}^{e+h/2} \rho\zeta^2 d\zeta.$$

We consider a material point Q at distance ζ from the reference surface of the shell and P its orthogonal projection on this surface. Denoting $\mathbf{n}_0$ the normal to the mean surface, the position vector $\boldsymbol{PQ}$ can be expressed as $\boldsymbol{PQ} = e\mathbf{n}_0$. One of the basic principles of semi-global methods (Ulm 1993a, Aouameur 1998, Ragueneau 1998) is to assume a constant stress state in each layer (resp. fiber) of the multilayered shell (resp. multifibered beam) to have a simple description of the local nonlinear behaviour. Considering a constant stress state in the section of the moved single-layer shell, the generalized forces at point P are written as functions of the curvature radii of the shell, R_α and R_β, and of the stress tensor at point Q:

$$\begin{aligned} \mathbf{N}_\alpha &= (\boldsymbol{\sigma}\cdot\mathbf{n}_\alpha)\left(h + \frac{eh}{R_\beta}\right) \\ \mathbf{N}_\beta &= (\boldsymbol{\sigma}\cdot\mathbf{n}_\beta)\left(h + \frac{eh}{R_\alpha}\right) \end{aligned} \tag{3}$$

$$\begin{aligned} \mathbf{M}_\alpha &= \mathbf{n}_0 \wedge (\boldsymbol{\sigma}\cdot\mathbf{n}_\alpha)\left(eh + \frac{h^3 + 12e^2h}{12R_\beta}\right) \\ \mathbf{M}_\beta &= \mathbf{n}_0 \wedge (\boldsymbol{\sigma}\cdot\mathbf{n}_\beta)\left(eh + \frac{h^3 + 12e^2h}{12R_\alpha}\right) \end{aligned} \tag{4}$$

Multiplying Eqs. (1) and (2) by $\hat{\mathbf{U}}_0$ and $\hat{\boldsymbol{\Omega}}_0$ (respectively), and after integration by parts of the result on S, we obtain the weak formulation of the dynamic balance Eqs. (1) and (2), of a moved single-layer shell:

$$\begin{aligned} \forall\hat{\mathbf{U}}_0, \forall\hat{\boldsymbol{\Omega}}_0 \quad & -\int_S B\mathbf{N}_\alpha\cdot\frac{\partial\hat{\mathbf{U}}_0}{\partial\alpha}dS - \int_S A\mathbf{N}_\beta\cdot\frac{\partial\hat{\mathbf{U}}_0}{\partial\beta}dS - \int_S B\mathbf{M}_\alpha\cdot\frac{\partial\hat{\boldsymbol{\Omega}}_0}{\partial\alpha}dS - \int_S A\mathbf{M}_\beta\cdot\frac{\partial\hat{\boldsymbol{\Omega}}_0}{\partial\beta}dS \\ & + \int_S AB(\mathbf{n}_\alpha\wedge\mathbf{N}_\alpha + \mathbf{n}_\beta\wedge\mathbf{N}_\beta)\cdot\hat{\boldsymbol{\Omega}}_0 dS + \int_S AB(\mathbf{q}\cdot\hat{\mathbf{U}}_0 + \mathbf{m}\cdot\hat{\boldsymbol{\Omega}}_0)dS \\ & -\int_S AB(\rho h\ddot{\mathbf{U}}_0\cdot\hat{\mathbf{U}}_0 + I\ddot{\boldsymbol{\Omega}}_0\cdot\hat{\boldsymbol{\Omega}}_0 + \rho eh\ddot{\mathbf{U}}_0\cdot\hat{\boldsymbol{\Omega}}_0 + \rho eh\ddot{\boldsymbol{\Omega}}_0\cdot\hat{\mathbf{U}}_0)dS = 0 \end{aligned} \tag{5}$$

This formulation is generalized to the multilayer case by superposition of n moved single-layer shells (compatibility of the shells displacements at global scale). For a multilayer shell element, this allows us to write the following incremental balance matricial equation:

$$[M]\{\ddot{\xi}_n\} + \sum_{k=1,n} [K(C^{ep})]_k\{\Delta\xi_n\} = \{F_{\text{ext}}\} - \sum_{k=1,n} \{F_{\text{int}}(\boldsymbol{\sigma})\}_k \tag{6}$$

where $\{\Delta\xi_n\}$ is the vector of nodal parameters increase at the considered iteration.

Eq. (6) raises the need for the computation of the tangent stiffness matrix as well as the internal forces vector for all the layers ($k = 1, n$). It leads to the following expression:

$$\begin{aligned} \sum_{k=1,n} [K(C^{ep})]_k &= \sum_{k=1,n} h_k \int_{S_k} [B]_k^t [C^{ep}]_k [B]_k dS_k \\ \sum_{k=1,n} \{F_{int}(\boldsymbol{\sigma})\}_k &= \sum_{k=1,n} h_k \int_{S_k} [B]_k^t [\boldsymbol{\sigma}]_k dS_k \end{aligned} \tag{7}$$

$[B]_k$ being the matrix of the derivatives of the interpolation functions linking the nodal displacement vector of the multilayer shell element to the components of local strain tensor for layer k.

Shell theory allows the use of plane stress assumption for the multilayer shell. This assumption states that the stress normal to the reference surface of the shell is zero. It is then necessary to fulfill this assumption in every single layer of the multilayer shell. A particular treatment of Eqs. (7a) and (7b) is needed for the computation of stresses as well as the tangent behaviour matrix $[C^{ep}]$ at the local scale of each layer.

4.2 Plane stress condition

For the integration of stresses, one considers a local iterative scheme (Ortiz 1986) allowing the use of various constitutive laws with internal variables. Whatever the constitutive law is, the computation of stresses is performed the same way (Aouameur 1998, 1999). For sake of simplicity in the presentation, one considers here the case of perfect plasticity. The stress tensor for the loading increment n at an integration point of layer k of the shell can be expressed as:

$$\boldsymbol{\sigma}_{n+1} = \boldsymbol{\sigma}_n + \mathbf{C}:(\Delta\boldsymbol{\varepsilon}_{n+1} - \Delta\lambda\partial_\sigma g_{n+1}) \quad \text{with} \quad \partial_\sigma g_{n+1} = \left.\frac{\partial g}{\partial \boldsymbol{\sigma}}\right|_{n+1} \tag{8}$$

$\Delta\boldsymbol{\varepsilon}_{n+1}$ is the total strain increment, g and $\Delta\lambda$ the plastic potential and multiplier (respectively).

Then, one defines a statically admissible tensor $\boldsymbol{\sigma}^*_{n+1}$ such as:

$$\boldsymbol{\sigma}^*_{n+1} = \mathbf{C}:\Delta\boldsymbol{\varepsilon}_{n+1} + \boldsymbol{\sigma}_n \tag{9}$$

Afterwards, one takes this stress tensor to verify the criterion, that is $f(\boldsymbol{\sigma}^*_{n+1}) \le 0$. If this condition is fulfilled, the statically admissible stress state is then located out of the loading surface; it is then necessary to make a plastic correction by projecting this stress state onto this surface. For this projection, one must verify both conditions on the criteria as well as for the plane stress assumption (that is: $\mathbf{n}_0 \cdot \boldsymbol{\sigma}_{n+1} \cdot \mathbf{n}_0 = 0$). This goal is reached thanks to a local iterative scheme, in which f is linearized at each iteration (k) and a plastic correction is computed:

$$\begin{aligned} f^{(k)}_{n+1} &= f^{(k-1)}_{n+1} + \partial_\sigma f^{(k-1)}_{n+1}:\delta\boldsymbol{\sigma}^{(k)} \\ &= f^{(k-1)}_{n+1} - \delta\boldsymbol{\lambda}^{(k)}\partial_\sigma f^{(k-1)}_{n+1}:\mathbf{C}:\partial_\sigma g^{(k-1)}_{n+1} = 0 \end{aligned} \tag{10}$$

The stress state obtained here is then corrected to satisfy the plane stress assumption (Aouameur 1998):

$$\boldsymbol{\sigma}_{n+1}^{(k)} = \boldsymbol{\sigma}_{n+1}^{(k-1)} - \delta\lambda^{(k)}\mathbf{C}:\partial_\sigma g_{n+1}^{(k-1)} - diag\left[\frac{\nu}{1-\nu}, \frac{\nu}{1-\nu}, 1\right]\delta\bar{\boldsymbol{\sigma}}_{zz}^{(k)} \tag{11}$$

ν is the Poisson's ratio and $\delta\bar{\boldsymbol{\sigma}}_{zz}^{(k)}$ the increase of $\bar{\boldsymbol{\sigma}}_{zz}$ for the plane strain solution. One performs local iterations until the criteria is below a given limit: $\left|f_{n+1}^{(k)}\right| \leq \mathrm{TOL}\left|f_{n+1}^{(0)}\right|$.

As for the integration of stresses, the plane stress assumption must be satisfied during the computation of the elastoplastic behaviour tensor used for the determination of the tangent rigidity matrix (7a). Therefore, we use a method proposed by De Borst (1991). Considering the stress tensor for the loading increment $(n + 1)$ under the following vectorial form:

$$\{\sigma\}_{n+1} = \{\sigma\}_n + [C^{ep}]_{n+1}\{\Delta\varepsilon\}_n \tag{12}$$

where $[C^{ep}]$ is the matrix representing the constitutive tangent tensor which is not taking into account the plane stress assumption.

The method proposed by De Borst considers the decomposition of the terms of Eq. (12) as follows:

$$\{\sigma\} = [\{\bar{\sigma}\}, \sigma_{zz}]^t; \{\Delta\varepsilon\} = [\{\Delta\bar{\varepsilon}\}, \Delta\varepsilon_{zz}]^t; \text{ and } [C^{ep}] = \begin{bmatrix} [C_{11}^{ep}] & [C_{12}^{ep}] \\ [C_{21}^{ep}] & (C_{22}^{ep}) \end{bmatrix} \tag{13}$$

The plane stress condition $\mathbf{n}_0 \cdot \boldsymbol{\sigma}_{n+1} \cdot \mathbf{n}_0 = 0$ allows the computation of the strain increment $(\Delta\varepsilon_{zz})_{n+1}$ through the following relation:

$$(\Delta\varepsilon_{zz})_{n+1} = -(C_{22}^{ep})_{n+1}^{-1}([C_{21}^{ep}]_{n+1}\{\Delta\varepsilon\}_{n+1} + (\sigma_{zz})_n) \tag{14}$$

Introducing Eqs. (13) and (14) in (12), it gives:

$$\begin{aligned} \{\bar{\sigma}\}_{n+1} &= \{\bar{\sigma}\}_n + [\bar{C}^{ep}]_{n+1}\{\Delta\bar{\varepsilon}\}_{n+1} \quad \text{with} \\ [\bar{C}^{ep}]_{n+1} &= \left[[C_{11}^{ep}]_{n+1} - \frac{[C_{12}^{ep}]_{n+1}[C_{21}^{ep}]_{n+1}}{(C_{22}^{ep})_{n+1}}\right] \end{aligned} \tag{15}$$

The expression of the elastoplastic constitutive matrix meeting the plane stress condition is then obtained through Eq. (15).

5. Analysis of the seismic response of the structure

5.1 General description

As shown in Figs. 1 and 3, the structure considered for the CAMUS international benchmark is composed of two parallel R/C walls without openings, linked by 6 square floors. Since there is a lateral bracing system, the parasite transversal motion should be very small and non-symetric failure

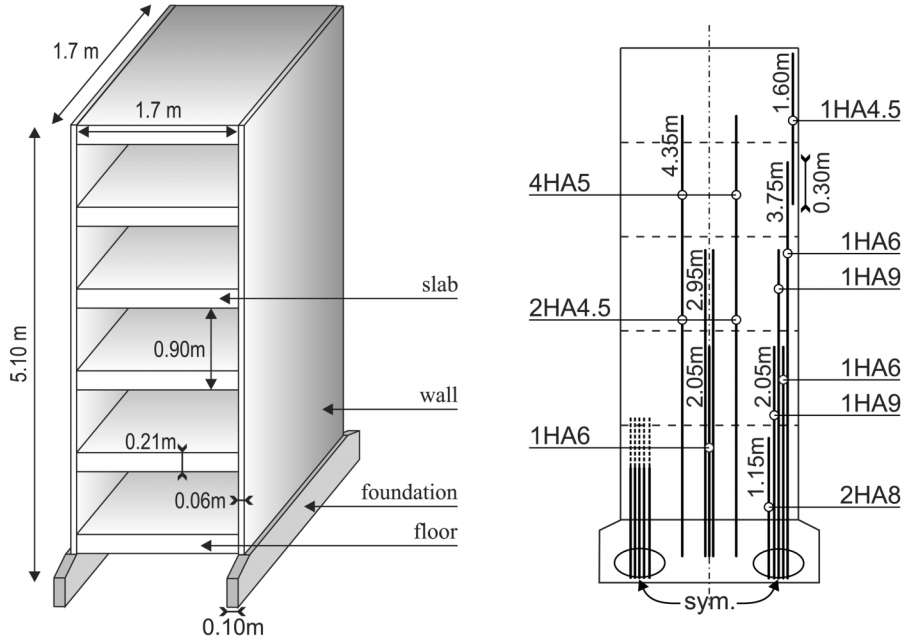

Fig. 3 Schematic of the Camus structure and members (left) and description of the reinforcements in the walls (right)

Table 1 Steel reinforcement at the level of each floor (CEA 1997)

Floor	Side of the walls	Central reinforcement
Level 6	$\Phi 4.5 = 15.9$ mm^2	No reinforcement
Level 5	$\Phi 4.5 = 15.9$ mm^2	$4\Phi 5 = 78.4$ mm^2
Level 4	$\Phi 6 = 28.3$ mm^2	$4\Phi 5 = 78.4$ mm^2
Level 3	$\Phi 6 + \Phi 8 + \Phi 4.5 = 94.4$ mm^2	$4\Phi 5 + 2\Phi 4.5 = 110.2$ mm^2
Level 2	$2\Phi 6 + 2\Phi 8 + 2\Phi 4.5 = 188.9$ mm^2	$4\Phi 5 + 2\Phi 4.5 + \Phi 6 = 138$ mm^2
Level 1	$4\Phi 8 + 2\Phi 6 + 2\Phi 4.5 = 289.4$ mm^2	$4\Phi 5 + 2\Phi 4.5 + \Phi 6 = 138$ mm^2

of the structural walls should be avoided. Both 2D and 3D modeling have then been considered in the study (Semblat 1998b) but the 2D results are not presented in this paper. All the data concerning the geometry, the material properties, the members are given in the Camus Benchmark Report "Mock-up and loading characteristics" (CEA 1997). As depicted in Fig. 3 (right) and detailed in Table 1, the mock-up has been reinforced considering the French PS92 seismic design code. New studies are in progress in the framework of the CAMUS project to take into account the EC8 code.

5.2 Preliminary modal analysis

The model is mainly built considering the modal properties of the structure (first three eigenmodes estimated from low level random excitation). The first experimental frequency of the mock-up was measured before the first tests equal to 7.24 Hz, the second one to around 33 Hz (in-plane bending)

and the first vertical eigenmode has a natural frequency equal to 20 Hz. The numerical analysis starts from this point and non linear material properties are introduced afterwards.

Since the mass of the structure is rather large (36 tons), one has to include in the model the shaking table itself as well as its supports (vertical springs). We consequently consider two complete models (2D and 3D) as depicted in Fig. 4 in the 3D case (structure + shaking table + vertical

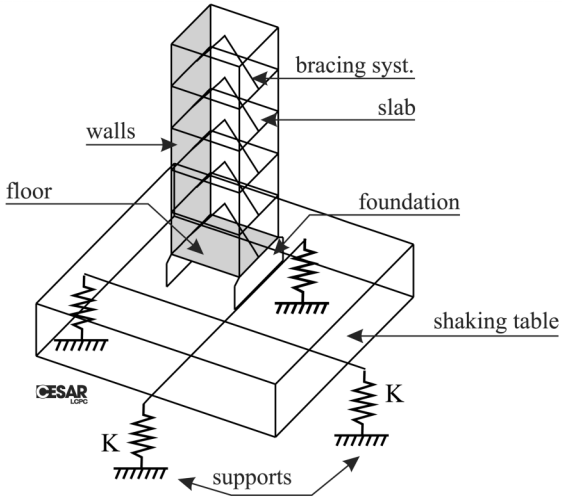

Fig. 4 Schematic of the complete model (table + structure + springs)

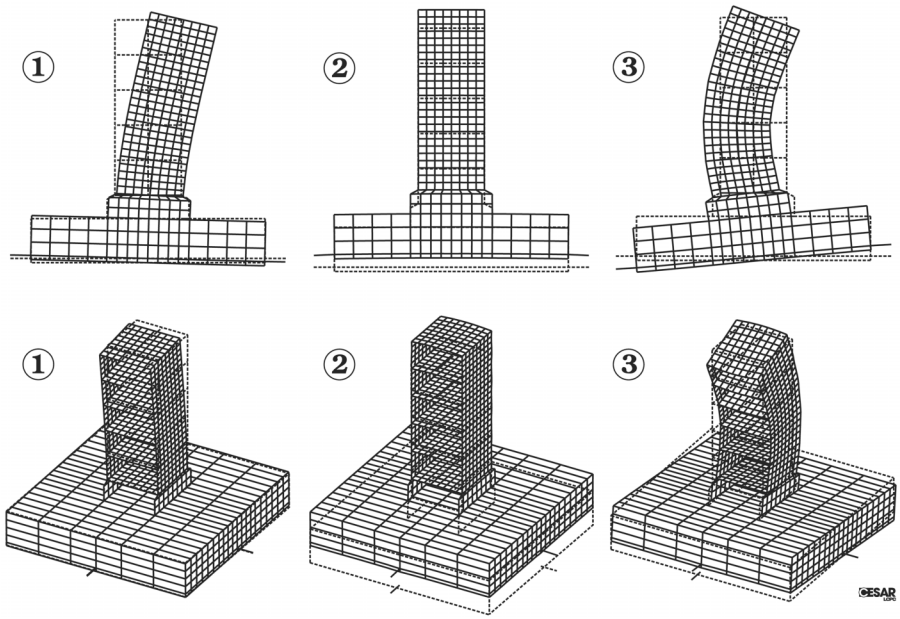

Fig. 5 First three eigenmodes of the table/structure system for both 2D and 3D models

springs). It is mainly composed of multilayered shell elements, tridimensional block and beam elements. The boundary condition concerns the centre of gravity which is fixed in the horizontal direction to avoid the free body motion of the structure. In the computation, the value of the stiffness of the four table vertical springs (Fig. 4) is $K = 3.0\ 10^8$ N/m.

The three first eigenmodes of the complete three-dimensional model (structure + shaking table) are given in Fig. 5. The first eigenmode corresponds to in-plane bending, the second one to pure vertical motion and the third one to another in-plane bending mode. The corresponding eigenfrequencies are the following :

- 2D case : 7.75 Hz, 20.43 Hz and 33.82 Hz,
- 3D case : 7.65 Hz, 19.58 Hz and 33.25 Hz.

The numerical results obtained are satisfactory and close to the experimental ones. The eigenfrequencies have a little discrepancy and the corresponding percentages of error are small : 7.0%, 2.0%, 2.4% (2D) and 5.6%, 2.1% and 0.07% (3D). For the non linear numerical computations, we have chosen both types of model (2D and 3D). Only the results obtained with the latter will be presented here to show the accuracy of the multilayered shell elements for this specific type of loading.

5.3 Linear dynamic response

The seismic response of the structure is firstly estimated in the linear case using the modal superposition method (Bisch 1999, Clough 1993). This response will be compared afterwards to the one obtained in the non linear case considering the multilayered shell element. The 3D linear model involves 5871 nodes and 1548 elements (linear shells, tridimensional blocks, springs (table supports) and beam elements).

Two different excitation signals are considered (CAMUS17 and CAMUS19) corresponding to acceleration levels of 0.40 g and 0.71 g. These acceleration signals are representative of the French design spectrum with the characteristics of a far field record. These signals are depicted in Fig. 6 and correspond to the horizontal acceleration applied to the shaking table. The loading of the structure is then equivalent to a rigid base motion. We then have considered a volumic density of force in the horizontal direction having the same variations in time than the applied acceleration. Inertial forces are directly involved in the computation giving the response to horizontal rigid base motion (Clough 1993). For the computation, 1200 time steps of $\Delta t = 0.01$ s are considered.

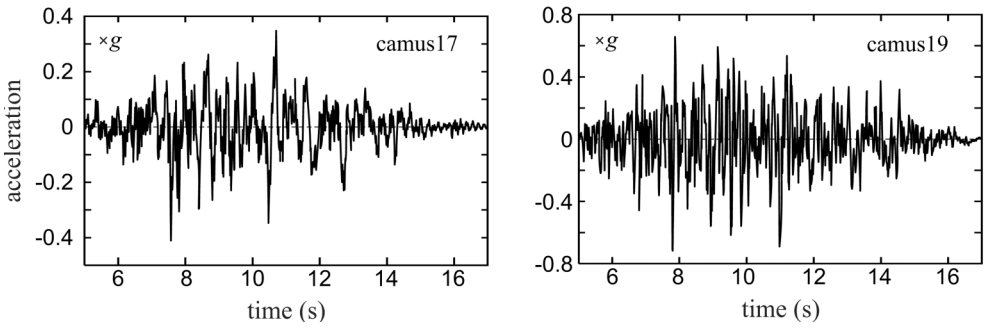

Fig. 6 Acceleration signals used in the shaking table tests

Table 2 Eigenfrequencies and effective modal masses

Mode number	Eigen freq. (Hz)	Effective modal mass (%)
1	7.75	41.59%
2	20.43	0.000%
3	33.82	10.18%
4	58.42	0.272%
5	63.62	0.000%
6	90.53	2.791%
7	129.71	0.000%
8	131.17	0.824%
9	164.13	0.444%
10	174.94	0.027%

Fig. 9 gives the horizontal displacement at the top of the structure obtained by modal superposition for the two acceleration signals (CAMUS17 and 19). It can be seen that this displacement increases with the signal magnitude. In fact, for CAMUS17, the maximum displacement is about 1.2 cm, whereas for CAMUS19, it is worth 5 cm. The linear modal response is compared afterwards with the non linear one. Table 2 gives the effective modal masses from the modal superposition computations (Clough 1993). Two modes are mainly contributing to the dynamic response of the structure : the first and the third ones with respective effective modal mass of 41% and 10%. The contribution of each of the other ten first modes to the dynamic response is actually negligible.

6. Non linear seismic response

6.1 Multilayered shell model

Fig. 7 shows the meshing of the three-dimensional model used in the non linear analysis. It is composed of multilayered shell elements, tridimensional blocks, springs (table supports) and beam elements. Because of the symmetry, only half of the structure is modelled. The 3D nonlinear model involves 1194 nodes and 906 elements. We consider here the same loadings than in the linear case (CAMUS17 and 19, Fig. 6). A macroscopic model (the Willam-Warnke model with 3 parameters) coupling plasticity with damage is used for modeling the non-linear behaviour of concrete (Willam 1973, Ulm 1993a). For the computation, 6000 time steps of $\Delta t = 0.002$ s are considered.

6.2 Constitutive law for concrete

The multilayered shell element allows the use of different constitutive laws in each layer. For the model presented in Fig. 7, the behaviour of concrete is considered through Willam-Warnke constitutive model with 3 parameters (Aouameur 1998, Ulm 1993a, 1994, Willam 1973). This criterion is depicted in Fig. 8 in the $\tau - \sigma$ plane as well as in the deviatoric plane. It is close to Drucker-Prager criterion but adapted to concrete for low hydrostatic pressures. The elasticity domain

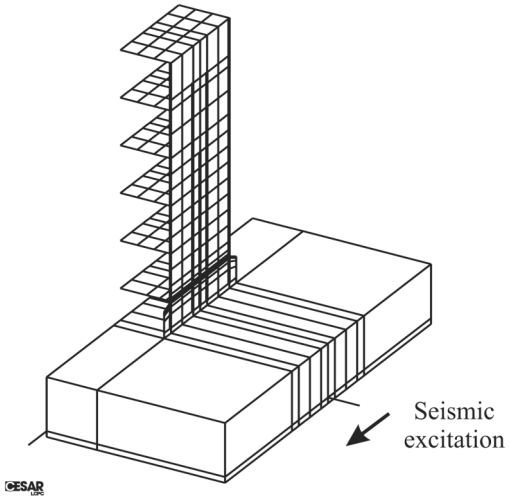

Fig. 7 Finite element mesh (non linear case)

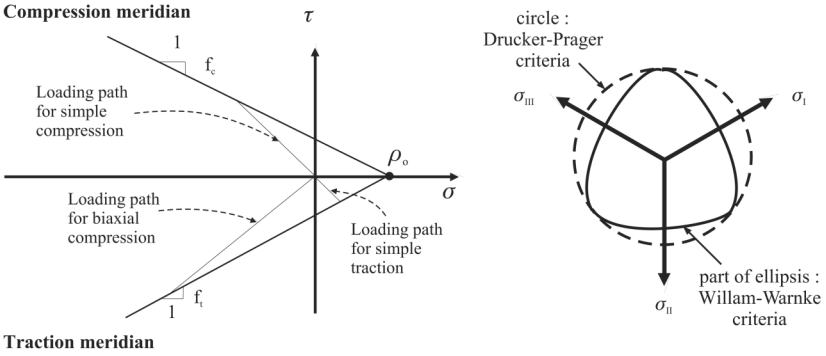

Fig. 8 Willam-Warnke criterion with 3 parameters in τ–σ plane

is a cone with a non circular section bounded by portions of an ellipsis between two meridians. The damage processes are also very important for the analysis of the behaviour of concrete (Mazars 1990). The extension of the Willam-Warnke model to damaging plasticity was proposed by Ulm (1993a, 1994). For the non linear computations, we consider this formulation of Willam-Warnke model. Some recent researches give another type of generalization of this model describing viscous hardening for the analysis of the fast dynamic behaviour of concrete (Sercombe 1998).

For the present analysis, the concrete walls are modelled with multilayered finite shell elements with 8 layers within their thickness. The influence of the number of layers in the shell has been studied in details by Aouameur (1998) and, to make an optimal choice, one has to recover the global flexural inertia of the shell as well as the whole stress state. Following the French PS92 seismic code, some few reinforcements (bars) are connected to the walls (CEA 1997, Quéval 1998) as depicted in Fig. 3 and synthetized in Table 1. For the non-linear behaviour of concrete in these multilayered shells, one considers the Willam-Warnke model with 3 parameters coupling plasticity with damage. The values of the constitutive parameters are chosen as follows:

- mass density = 2400 kg/m^3
- Young's modulus = 28000 MPa
- Poisson's ratio = 0.2
- thickness of the wall = 0.06 m
- compression strength F_c = 30 Mpa
- tensile strength F_t = 2.5 Mpa
- biaxial compressive strength F_{bc} = 33 MPa
- yield strength A_o = 1
- ultimate strength B_o = 0.01
- softening factor = 7500
- damaging factor = 5000
- ultimate Young modulus $E_{ultimat}$ = 28 Mpa

6.3 Non linear dynamic response and frequency drop

Fig. 9 gives the horizontal displacement at the top of the structure for the two acceleration signals : CAMUS17 and 19. The non linear dynamic response (blind simulation) obtained is compared to the linear one. These responses coincide during the first time steps and there is afterwards a large discrepancy when non linear effects due to concrete cracking appear. It shows the influence of local damage on the dynamic response of the whole structure. It leads to a strong increase of the period of vibration of the structure, that is a frequency drop (Ulm 1993b). For CAMUS19, the values are as follows:

- *linear case* : the main frequency in the response signal is 7.62 Hz which very close to the first eigenfrequency of the system,
- *nonlinear case* : the fundamental frequency of the dynamic response is 2.25 Hz showing a very large softening of the structure for such a strong motion.

Since the seismic loading is an in-plane excitation, some comparisons were made between 2D and multilayered shell model for the non-linear response (Semblat 1998b, 1999). The agreement between both solutions is very good, the 2D model giving nevertheless displacements a little bit smaller than in the 3D case. The advantage of the multilayered shell formulation is to allow any other type of 3D seismic excitation (out of plane, torsion...).

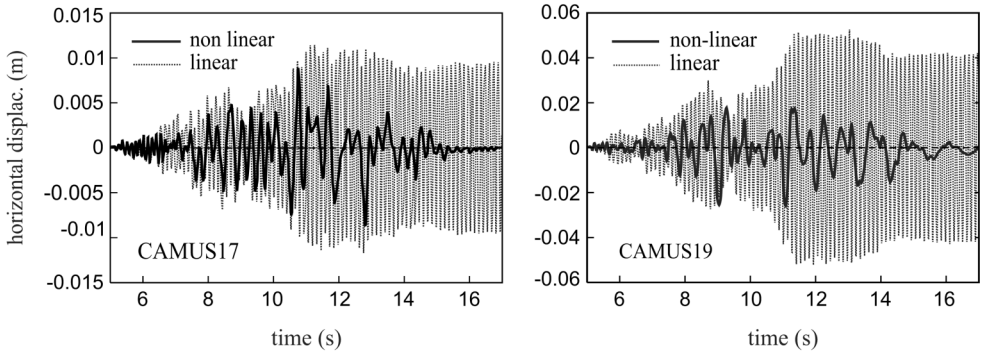

Fig. 9 Horizontal displacements at the top of the structure in both linear and non linear cases

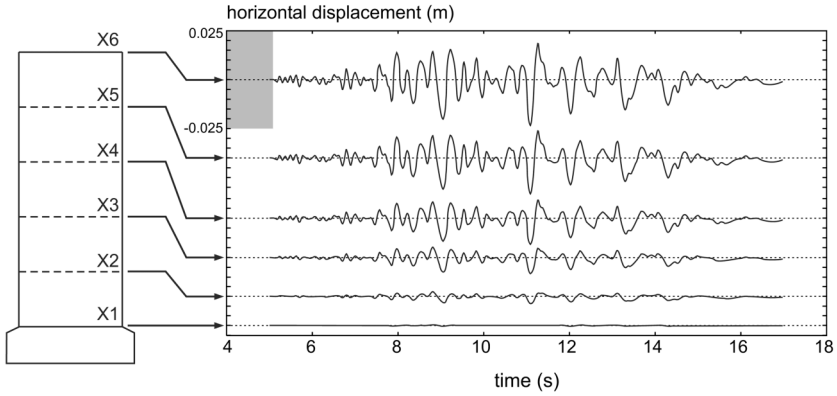

Fig. 10 Horizontal displacement at each level of the structure (CAMUS19, 0.71 g)

6.4 Dynamic response at each level

Fig. 10 gives the computed horizontal displacements at each level of the structure for seismic excitation CAMUS19 (0.71 g). For each signal, the frequency drop estimated earlier can be noticed. The displacement at level 1 is very small and it increases rather fastly for levels 2 and 3 showing that the non linear dynamic response of the structure is qualitatively rather different from its first eigenmode mainly governing the linear response. For the nonlinear dynamic responses of Fig. 10, the maximum displacements at the top is 0.025 m, 0.020 m for level 5 and 0.015 m for level 4. For the first levels, the displacements are much smaller and we will analyze in the next subsection the corresponding strains.

6.5 Vertical strains at each level

Since the nonlinear strains may appear at the first levels, we display in Fig. 11 the vertical strains

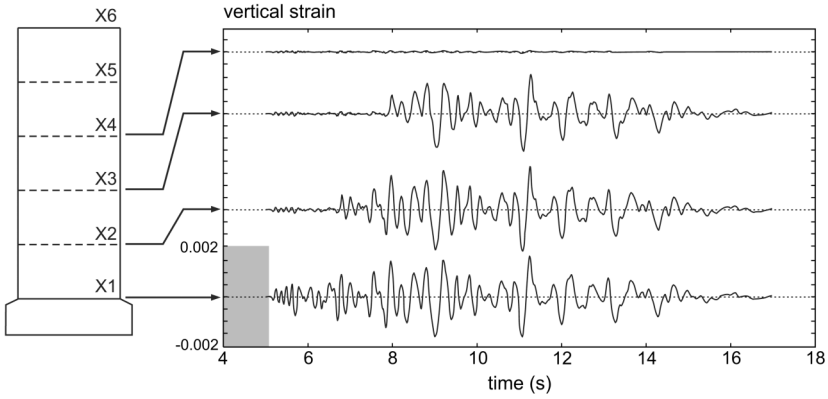

Fig. 11 Vertical strain ε_{yy} at each level of the structure (CAMUS19, 0.71 g)

on the lateral part of the walls versus time for the seismic excitation CAMUS19 (0.71 g). As shown by the vertical strain at level 1, the damaging of the structure at this level appears at the beginning of the loading. Before t = 7 s, the vertical strain at levels 2, 3 and 4, remains very small. At level 2, the increase in vertical strain (plastic strain) is significant between 7 and 8 s and above 8 s for level 3. The vertical strain at level 4 remains very small when compared to the other levels and it seems that there is no plastic strain at level 4. We will see afterwards computed plastic strain patterns and mock-up actual crack patterns.

7. Comparisons with experiments

7.1 Non linear dynamic response : numerical vs experimental results

To analyze the accuracy of the multilayered finite shell element, we compare the numerical results from the blind simulations made for the benchmark to the final experimental results given afterwards to the participants (CEA 1998). For the seismic excitation CAMUS19 (0.71 g), Fig. 12 gives the top horizontal displacements for the experiments and the 3D computations (original blind simulation). First of all, the frequency-drop is very well reproduced showing a strong lengthening of the period of the dynamic response. Secondly, the larger displacement peaks are very well recovered in the negative part of the curve. Thirdly, the computed top displacement still underestimates the actual response. This is mainly due to the fact that the same mock-up was used for low and moderate excitation experiments first (CAMUS02/0.24 g and CAMUS17/0.40 g) and this loading history was not taken into account in the numerical model. Considering this drawback of the model, the comparison between the experimental results and the blind simulation results is very satisfactory in terms of frequency-drop as well as maximum displacement peaks. The multilayered finite shell element could then be used for future simulation with other types of excitations.

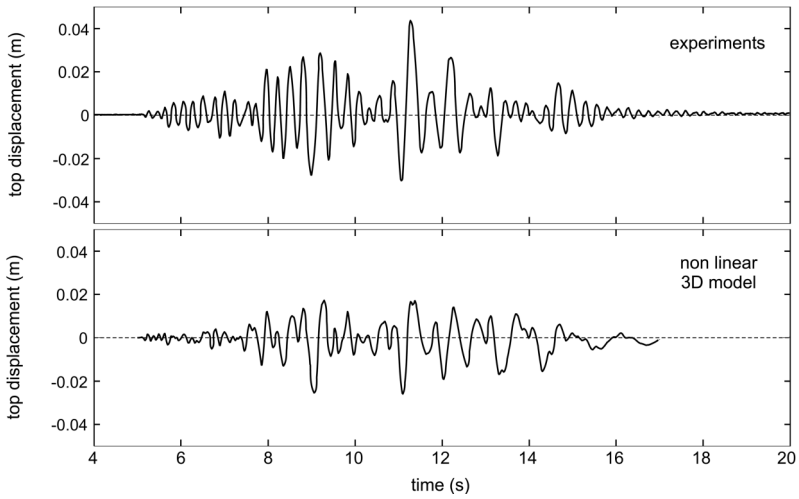

Fig. 12 Measured and computed top horizontal displacements (CAMUS19)

7.2 Analysis of plastic strains and comparison with crack patterns

Fig. 13 gives the plastic strain isovalues at time t = 11 s for the two acceleration signals : CAMUS17 and 19. These isovalues show the increase of plastic strains with the signal magnitude. For the first acceleration signal (CAMUS17, 0.40 g), only the first level and the bottom of the second one have significant plastic strains on their lateral parts. For the strongest accelerogram CAMUS19 (0.71 g), the three first levels show large plastic strain corresponding to a strong damaging of the concrete. This results is in good agreement with the vertical strain curves given in the previous section : no plastic strain appears above level 3.

It is possible to make a qualitative comparison between the computed plastic strains isovalues (Fig. 13) and the actual crack pattern observed for Camus 19 test (Fig. 14). On both figures, plastic strains as well as cracking are large for the two first levels. Computed plastic strains and observed cracks are mainly located on the lateral parts of the walls and are larger near the corners. From the

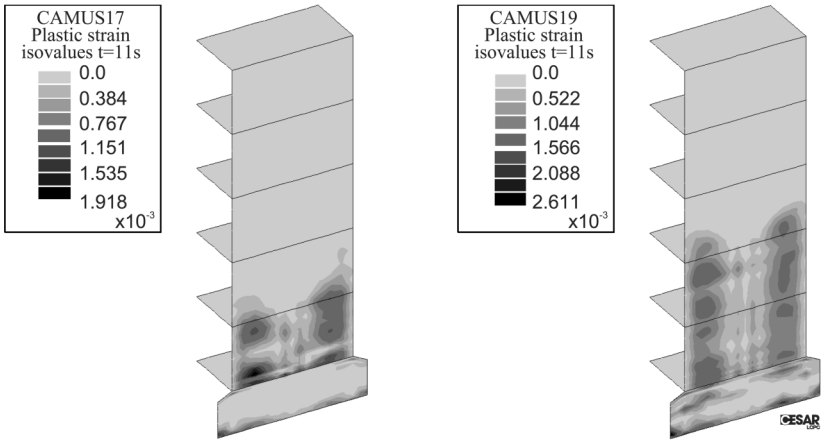

Fig. 13 Plastic strains at time t = 11s (Camus 17 and 19)

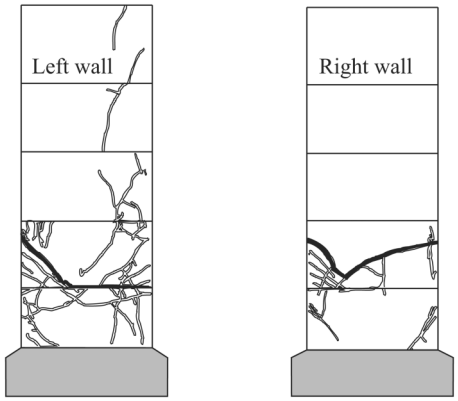

Fig. 14 Crack pattern on both left and right walls after Camus 19 test (CEA, 1998)

qualitative point of view, the numerical computations give a good idea of the local plastic strain distribution at the two first levels. As found in both numerical and experimental results, plastic strains and damage are small for the three top levels.

8. Conclusions

In the CAMUS project, the seismic response of a building was studied through shaking table tests on a reduced-scale model (CEA 1997, Quéval 1998). The contribution of the LCPC to the numerical benchmark of the project (blind simulation) has been made considering a multilayered shell model.

Numerical results obtained through non linear dynamic response clearly show the efficiency and accuracy of the proposed multilayered shell element formulation for this simple in-plane type of excitation. This formulation allows the computation of the non linear dynamic response of complex three-dimensional structures under severe seismic loadings. Furthermore it is made in a general frame and one can choose any constitutive law for the different materials (Aouameur 1998, 1999). In this paper, computations under seismic loading were performed considering, for the concrete, a constitutive model within the frame of damaging plasticity. The numerical results (blind simulation) obtained with the multilayered shell formulation are satisfactory when compared to experimental results from shaking table tests. Furthermore they give interesting and realistic information about the global and local behaviour of the structure.

Comparisons between the numerical results obtained by the different participants with various numerical methods were proposed by the CEA (CEA 1998). Detailed numerical results are also given in (Ragueneau 1998, Ile 1998).

Acknowledgements

The authors gratefully acknowledge the help of Dr. H. Mitani who, during his internship at LCPC in 1998, contributed to the simulations.

References

Aouameur, A. (1998), “Non linear material and geometrical analysis of RC shell structures under static and dynamic loadings (in French)”, Ph.D. thesis, ENPC, Paris.

Aouameur, A., Ulm, F.J., Humbert, P. and Semblat, J.F. (1999), “Non linear structural analysis by multilayered shell elements (in French)”, *Revue Française de Génie Civil*, **3**(5), 219-238.

Aubry, D. and Modaressi, H. (1992), “Seismic wave propagation in soils including non-linear and pore pressure effects”, *Recent Advances in Earthq. Eng. Struct. Dyn.*, V. Davidovici ed., 209-224.

Bard, P.Y. and Bouchon, M. (1985), “The two-dimensional resonance of sediment-filled valleys”, *Bull. Seismological Society of America*, **75**(2), 519-541.

Bisch, P., Langeoire, A., Prat, M. and Semblat, J.F. (1999), *Structures in Interaction (Finite elements in civil engineering)*, Chap.7 : Modelling of structures in seismic areas - wave propagation, Hermes ed., 467-562.

CEA (1997), *Mock-up and Loading Characteristics. Specifications for the Participants Report*, « Camus » International Benchmark.

CEA (1998), *Synthesis of the Participants Reports*, « Camus » International Workshop, *11th European*

Conference on Earthquake Engineering, Paris, Balkema ed.
Chopra, A.K. and Goel, R.K. (2002), "A modal pushover analysis procedure for estimating seismic demands for buildings", *Earthq. Eng. Struct. Dyn.*, **31**, 561-582.
Clough, R.W. and Penzien, J. (1993), *Dynamics of Structures*, Mc Graw-Hill.
De Borst, R. (1991), "The zero-normal-stress condition in plane-stress and shell elastoplasticity", *Communication in Applied Numerical Methods*, **7**, 29-33.
Fajfar, P. (2000), "A nonlinear analysis method for performance-based seismic design", *Earthquake Spectra*, **16**(9), 573-592.
Garnier, J. and Pecker, A. (1999), "Use of centrifuge tests for the validation of innovative concepts in foundation engineering", *2nd Int. Conf. on Earthquake Geotechnical Eng.*, 433-439, Lisbon.
Guéguen, P., Bard, P.Y. and Semblat, J.F. (2000), "From soil-structure to site-city interaction", *12th World Conf. on Earthq. Eng.*, Auckland, New Zealand.
Humbert, P. (1989), "CESAR-LCPC : a general finite element code (in French)", *Bulletin des Laboratoires des Ponts & Chaussées*, **160**, 112-115.
Igusa, T., Der Kiurehian, A. and Sackman, J.L. (1984), "Modal decomposition method for stationary response of non-classically damped systems", *Earthq. Eng. Struct. Dyn.*, **12**, 121-136.
Ile, N., Reynouard, J.M. and Merabet, O. (1998), "Seismic behaviour of slightly reinforced shear wall structures", *11th European Conf. on Earthq. Eng.*, Paris, Balkema ed.
Lin, C.S. and Scordelis, A.C. (1975), "Nonlinear analysis of RC shells of general form", *J. Struct. Div.*, ASCE, **101**, 523-538.
Luco, J.E. and Wong, H.L. (1986), "Response of a rigid foundation to a spatially random ground motion", *Earthq. Eng. Struct. Dyn.*, **14**, 891-908.
Mazars, J. (1998), "French advanced research on structural walls : An overview on recent seismic programs", *11th European Conf. on Earthq. Eng.*, Paris.
Mazars, J., Berthaud, Y. and Ramtani, S. (1990), "The unilateral behaviour of damaged concrete", *Engineering Fracture Mechanics*, **35**(4/5), 629-635.
Ortiz, M. and Simo, J.C. (1986), "An analysis of a new class of integration algorithms for elastoplastic constitutive relations", *Int. J. Numer. Meth. Eng.*, **23**, 353-366.
Pauley, T. and Priestley, M.J.N. (1992), *Seismic Design of Reinforced Concrete and Masonry Buildings*, Wiley.
Polak, M.A. and Vecchio, F.J. (1993), "Nonlinear analysis of reinforced-concrete shells", *J. Struct. Eng.*, **119**(12), 3439-3462.
Quéval, J.C., Combescure, D., Sollogoub, P., Coin, A. and Mazars, J. (1998), "CAMUS experimental program in-plane seismic tests of 1/3rd scaled R/C bearing walls", *11th European Conf. on Earthq. Eng.*, Paris.
Ragueneau, F. and Mazars, J. (1998), "Damping and boundary conditions : two major points for the description of the seismic behaviour of R/C structures", *11th European Conf. on Earthq. Eng.*, Paris, Balkema ed.
Seed, H.B., Wong, R.T., Idriss, I.M. and Tokimatsu, K. (1986), "Moduli and damping factors for dynamic analyses of cohesionless soils", *J. Geotechnical Engineering*, **112**(11), 1016-1032.
Semblat, J.F. (1997), "Rheological interpretation of Rayleigh damping", *J. Sound Vib.*, **206**(5), 741-744.
Semblat, J.F. and Luong, M.P. (1998a), "Wave propagation through soils in centrifuge testing", *J. Earthq. Eng.*, **2**(1), 147-171.
Semblat, J-F, Aouameur, A., Mitani, H., Ulm, F.J. and Humbert, P. (1998b), *CAMUS International Benchmark : Final Report*, Lab. Central des Ponts et Chaussées, 61.
Semblat, J.F., Aouameur, A., Ulm, F.J. and Mitani, H. (1999), "Seismic response of a building : the CAMUS project (in French)", *Bulletin des Laboratoires des Ponts et Chaussées*, **219**, 53-67.
Semblat, J.F., Duval, A.M. and Dangla, P. (2000), "Numerical analysis of seismic waves amplification in Nice (France) and comparisons with experiments", *Soil Dyn. Earthq. Eng.*, **19**(5), 347-362.
Semblat, J.F., Kham, M., Kurose, A., Xiao, H.H. and Dangla, P. (2002a), "Wave/cavity interaction : analytical and BEM approaches", *12th European Conf. on Earthq. Eng.*, London, 9-13 sept.
Semblat, J.F., Guéguen, P., Kham, M. and Bard, P.Y. (2002b), "Site-city interaction at local and global scales", *12th European Conf. on Earthq. Eng.*, London, 9-13 sept.
Sercombe, J., Ulm, F.J. and Toutlemonde, F. (1998), "Viscous hardening plasticity for concrete in high rate dynamics", *J. Eng. Mech.*, ASCE, **124**, 1050-1057.

Thomas, J.J., Luong, M.P. and Semblat, J.F. (1995), "Vibratory signature of electric pylons under impulse testing", *Smart Structures and Materials : Smart Systems for Bridges, Structures and Highways (SPIE/ASME)*, San Diego, **2446**, 258-267.

Ulm, F.J. and Guggenberger, J.M. (1993a), "3D non-linear time-dependent analysis of RC and PC beams", *5th RILEM Int. Symposium on Creep and Shrinkage of Concrete*, Bazant, Z.P. and Carol, I. eds, Chapman & Hall, London, 573-578.

Ulm, F.J., Clément, J.L. and Argoul, P. (1993b), "Coefficient de comportement : approche chute de fréquence", *3ème Colloque National en génie parasismique, Saint-Rémy-lès-Chevreuse*, 49-56.

Ulm, F.J. (1994), "Elastoplastic modelling including damage for structural concrete (in French)", Ph.D. thesis, ENPC, Paris.

Willam, K.J. and Warnke, E.P. (1973), "Constitutive model for the triaxial behavior of concrete", *International Association of Bridge and Structural Engineers, Seminar on Concrete Structures Subjected to Triaxial Stresses*, paper III-1, Bergamo, Italy, IABSE Proc.19.